

# Detection of Stellar Spots from the Observations of Caustic-Crossing Binary-Lens Gravitational Microlensing Events

Cheongho Han

Department of Astronomy & Space Science,  
Chungbuk National University, Chongju, Korea 361-763  
cheongho@astronomy.chungbuk.ac.kr

Ho-Il Kim

Korea Astronomy Observatory,  
Taejon, Korea 305-348  
hikim@hanul.issa.re.kr

Kyongae Chang

Department of Physics,  
Chongju University, Chongju, Korea 360-764  
kchang@alpha94.chongju.ac.kr

Sung-Hong Park

Department of Astronomy & Space Science,  
Chungbuk National University, Chongju, Korea 361-763  
parksh@astronomy.chungbuk.ac.kr

## ABSTRACT

Recently, Heyrovský & Sasselov (1999) investigated the sensitivity of *single-lens* gravitational microlensing event light curves to small spots and found that during source transit events spots can cause deviations in amplification larger than 2%, and thus be detectable. In this paper, we explore the feasibility of spot detection from the observations of *caustic-crossing binary-lens* microlensing events instead of single-lens events. For this we investigate the sensitivity of binary-lens event light curves to spots and compare it to that of single-lens events. From this investigation, we find that during caustic crossings the fractional amplification deviations of microlensing light curves from those of spotless source events are equivalent to the deviations of single-lens events, implying that spots can also be detected with a similar photometric precision to that required for spot detection by observing single-lens events. We discuss the relative advantages of observing caustic-crossing binary-lens events over the observations of single-lens events in detecting stellar spots.

*Subject headings:* gravitational lensing – stars: spots – photometry

submitted to *Monthly Notices of the Royal Astronomical Society*: Jul 19, 1999

Preprint: CNU-A&SS-07/99

## 1. Introduction

Massive searches for gravitational microlensing events by monitoring transient brightening of source stars located in the Galactic bulge and the Magellanic Clouds have been and are being carried out by several groups (EROS: Aubourg et al. 1993; MACHO: Alcock et al. 1993; OGLE: Udalski et al. 1993; DUO: Alard & Guibert 1997). These surveys have detected  $\sim 400$  events to date (Stubbs 1999).

The light curve of a single-lens microlensing event (denoted by the subscript ‘s’) with a point source (denoted by the subscript ‘0’) is given by

$$A_{s,0} = \frac{u^2 + 2}{u(u^2 + 4)^{1/2}}, \quad (1.1)$$

where  $u$  is the lens-source separation in units of the angular Einstein ring radius  $\theta_E$ . The angular Einstein ring radius is related to the physical parameters of the lens by

$$\theta_E = \left( \frac{4GM}{c^2} \frac{D_{ls}}{D_{ol}D_{os}} \right)^{1/2}, \quad (1.2)$$

where  $M$  is the lens mass and  $D_{ol}$ ,  $D_{ls}$ , and  $D_{os}$  are the separations between the observer, lens, and source star, respectively. Typical main-sequence stars in the Galactic bulge have radii that subtend only  $\lesssim 1 \mu$ -arcsecond, while the angular Einstein ring radius of an event caused by a solar mass lens with  $D_{ol} \sim 5$  kpc is  $\theta_E \sim 0.3$  milli-arcsecond. Therefore, equation (1.1) is a good approximation for majority of Galactic microlensing events.

However, for a very close lens-source impact event with a considerable source star radius such as subgiants and giants, the source can no longer be approximated by a point source. For this case, different parts of the source are amplified by different amounts (differential amplification) due to the finite size of the source star and the resulting light curve deviates from the point-source one (Schneider & Weiss 1986; Witt & Mao 1994). The light curve of an extended source event caused by a single lens is given by the intensity-weighted amplification averaged over the surface of the source star, i.e.

$$A_s(r_*) = \frac{\int_0^{2\pi} \int_0^{r_*} I(r, \vartheta) A_{s,0}(|\mathbf{r} - \mathbf{r}_L|) r dr d\vartheta}{\int_0^{2\pi} \int_0^{r_*} I(r, \vartheta) r dr d\vartheta}, \quad (1.3)$$

where  $r_*$  is the radius of the source star,  $I(r, \vartheta)$  is the surface intensity distribution of the source star, and the vectors  $\mathbf{r}_L$  and  $\mathbf{r} = (r, \vartheta)$  represent the displacement vector of the center of the source star with respect to the lens and the orientation vector of a point on the source star surface with respect to the source center, respectively.

By observing the distortions in microlensing light curves caused by the finite source effect, one can obtain useful information about both the lens and source star. First, it was known that finite source effect can be used to determine  $\theta_E$ , with which one can partially break the lens parameter degeneracy in the obtained Einstein time scale  $t_E$  (Gould 1994;

Nemiroff & Wickramasinghe 1994; Maoz & Gould 1994; Peng 1997). Second, since different parts of the source star (with varying surface intensity and spectral energy distribution) are resolved at different times during an event, one can recover the intensity profile of the source (Witt 1995; Loeb & Sasselov 1995; Gould & Welch 1996) and can probe stellar atmosphere (Valls-Gabaud 1994, 1998; Sasselov 1997; Gaudi & Gould 1999) by taking a sequence of photometric and spectro-photometric measurements of the event.

Recently, Heyrovský & Sasselov (1999) investigated the sensitivity of *single-lens* microlensing event light curves to small spots with radii  $r_s \lesssim 0.2$  of source radii. From this investigation, they found that during source transit events spots can cause deviations in amplification larger than 2%, and thus be detectable. In this paper, we explore the feasibility of spot detection from the observations of *caustic-crossing binary-lens* microlensing events instead of single-lens events. For this we investigate the sensitivity of binary-lens event light curves to spots and compare it to that of single-lens events. From this investigation, we find that during caustic crossings the fractional amplification deviations of microlensing light curves from those of spotless source events are equivalent to the deviations of single-lens events, implying that spots can also be detected with a similar photometric precision to that required for spot detection by observing single-lens events. We discuss the relative advantages of observing caustic-crossing binary-lens events over the observations of single-lens events in detecting stellar spots.

## 2. Single-Lens Events for Finite Source Stars with Spots

If the surface of a source star is maculated by a spot, the light curve of a single-lens microlensing event becomes

$$A_{s,\text{spot}} = \frac{\int_0^{2\pi} \int_0^{r_*} I(r, \vartheta) A_{s,0}(|\mathbf{r} - \mathbf{r}_L|) r dr d\vartheta - \int_{\Sigma_{\text{spot}}} f(\mathbf{r}') I(\mathbf{r}') A_{s,0}(|\mathbf{r}' - \mathbf{r}_L|) d\Sigma_{\text{spot}}}{\int_0^{2\pi} \int_0^{r_*} I(r, \vartheta) [1 - f(r, \vartheta)] r dr d\vartheta}, \quad (2.1)$$

where  $\mathbf{r}'$  is the orientation vector of a point on the surface of the spot with respect to the source center,  $f(\mathbf{r}')$  represents the fractional decrement in the surface intensity due to the spot, and the notation  $\int_{\Sigma_{\text{spot}}} \cdots d\Sigma_{\text{spot}}$  represents the surface integral over the spot range of the source star.

Due to the presence of the spot, the event light curve deviates from that of a spotless event. To see the pattern of the deviations in microlensing light curves caused by spots and to explore the feasibility of spot detection by this method, we compute the fractional amplification deviation in the light curve from that of a spotless event, i.e.

$$\epsilon_s = \frac{|A_{s,\text{spot}} - A_s|}{A_s}, \quad (2.2)$$

by using equations (1.3) and (2.1). For the computation of  $\epsilon_s$ , we assume a constant surface brightness of  $I_*$  for the entire region of the source star outside the spot. Partially, this is

because the limb darkening does not have significant effect on the light curve, but more importantly because we want to see the deviation caused solely by the spot. The spot is modeled by a circular area with a radius  $r_{\text{spot}}$  and also has a uniform surface brightness  $I_{\text{spot}}$ . We test two cases of events for which the source stars have radii of  $r_* = 0.05\theta_E$  and  $0.1\theta_E$ . For both cases, the spots have relative radii of  $r_{\text{spot}}/r_* = 0.2$  with the surface brightness contrast parameter of  $\mathcal{C} = I_*/I_{\text{spot}} = 1/(1 - f) = 10$ . With these assumptions, the light curve in equation (2.1) is simplified into

$$A_{\text{s,spot}}(r_*, r_{\text{spot}}, f) = \frac{\int_0^{2\pi} \int_0^{r_*} A_{\text{s},0}(|\mathbf{r} - \mathbf{r}_L|) r dr d\vartheta - f \int_0^{2\pi} \int_0^{r_{\text{spot}}} A_{\text{s},0}(|\mathbf{r}' - \mathbf{r}_L|) r' dr' d\vartheta'}{\pi(r_*^2 - f r_{\text{spot}}^2)}. \quad (2.3)$$

In the upper panels of Figure 1, we present the contours of the deviation  $\epsilon_s$  as a function of the *lens* position  $(x_L, y_L)$ . In each panel, the two circles represent the source star (big empty circle centered at the origin) and the stellar spot on it (small filled circle), respectively. The spot is located at  $s = 0.5r_{\text{spot}}$  from the center of the source star. Contours are drawn with a spacing of 0.2% from  $\epsilon_s = 0.2\%$  and the regions with  $\epsilon_s \geq 1\%$  and  $\epsilon_s \geq 2\%$  are shaded by darkening gray tones. In the lower panels, we also present several example light curves of events for source stars with (solid lines) and without spots (dotted lines) and the corresponding lens trajectories (dot-long dashed lines) are marked in the upper panels. Each pair of the trajectory and the corresponding light curve are marked by the same number. We note that our Figure 1 is equivalent to Figure 1 and 2 of Heyrovský & Sasselov (1999), except that their adopted source size is  $r_* = \theta_E/13.23$  and all their lengths are scaled by the source size not by the angular Einstein ring radius.

From the figure, one finds that the deviation can be larger than 2% as noted by Heyrovský & Sasselov (1999), and thus spots can, in principle, be detectable. However, the region for noticeable deviations (e.g.  $\epsilon_s \geq 2\%$ ) is confined to a very small localized area close to the spot. Even for source-transit events, unless the lens almost directly crosses the spot, the deviations will not be big enough to notice the existence of the spot. This implies that with a reasonable photometric precision, spots can be detected only for a very limited number of (almost) direct spot-transit events.

### 3. Caustic-Crossing Binary-Lens Events for Finite Source Stars with Spots

In previous section, we investigated the effect of stellar spots on the light curves of single-lens microlensing events. In this section, we investigate how the spots of source stars affect the light curves of caustic-crossing binary-lens events.

When lengths are normalized to the *combined* Einstein ring radius  $r_E$ , which is equivalent to the Einstein ring radius of a single lens with a mass equal to the total mass of the binary, the lens equation in complex notations for a binary-lens system with a point source is given by

$$\zeta = z + \frac{m_1}{\bar{z}_1 - \bar{z}} + \frac{m_2}{\bar{z}_2 - \bar{z}}, \quad (3.1)$$

where  $m_1$  and  $m_2$  are the mass fractions of individual lenses (and thus  $m_1 + m_2 = 1$ ),  $z_1$  and  $z_2$  are the positions of the lenses,  $\zeta = \xi + i\eta$  and  $z = x + iy$  are the positions of the source and images, and  $\bar{z}$  denotes the complex conjugate of  $z$  (Witt 1990). The amplification of each image,  $A_i$ , is given by the Jacobian of the transformation (3.1) evaluated at the images position, i.e.

$$A_{b,0,i} = \left( \frac{1}{|\det J|} \right)_{z=z_i} ; \quad \det J = 1 - \frac{\partial \zeta}{\partial \bar{z}} \frac{\partial \bar{\zeta}}{\partial z}. \quad (3.2)$$

Then the total amplification of a binary-lens event (denoted by the subscript ‘b’) with a point source is given by the sum of the amplifications of the individual images, i.e.  $A_{b,0} = \sum_i A_{b,0,i}$ . The set of source positions with infinite amplifications, i.e.  $\det J = 0$ , form closed curves called caustics. Therefore, whenever a point source crosses the caustic, the amplification becomes formally infinity, producing a sharp peak in the light curve. Since the caustics form a closed figure, the source transit occurs at least twice for a caustic-crossing binary-lens event.

The finite source effect also affects the light curves of binary-lens events. The light curve of a binary-lens event with a finite source,  $A_b$ , is obtained in a similar fashion to the single-lens event case, i.e. the intensity-weighted amplification averaged over the surface of the source star as is in equation (1.3) except that the single-lens point-source amplification  $A_{s,0}$  should be replaced by the binary-lens amplification for a point source  $A_{b,0}$ . Due to the finite source effect, the observed amplification remains finite even during the caustic crossings.

If a spot exists on the surface of a finite source, the light curve further deviates from  $A_b$ . The amplification of the binary-lens event for a source star with a spot,  $A_{b,\text{spot}}$ , is obtained by using equation (2.3), but with  $A_{b,0}$  instead of  $A_{s,0}$ . To see how the light curves of binary-lens events are affected by spots and to explore the feasibility of using binary-lens events for spot detection, we compute the fractional deviation in the amplification from that of a spotless event by

$$\epsilon_b = \frac{|A_{b,\text{spot}} - A_b|}{A_b}, \quad (3.3)$$

and the result is presented in Figure 2. In the upper panel of Figure 2, we present the contours of  $\epsilon_b$  in the vicinity of the caustics of an example binary-lens system with a binary separation (normalized by  $\theta_E$ ) and mass ratio of  $a = 1.0$  and  $q = 1.0$ , respectively. The closed figure (marked by thick solid curves) in each panel represents the caustics of the binary-lens system. The contours are drawn at the levels of  $\epsilon_b = 1\%$  and  $2\%$  and the regions with  $\epsilon_b \geq 1\%$  and  $\epsilon_b \geq 2\%$  are shaded by darkening gray tones. For direct comparison of the deviations to those of the single-lens events in Figure 1, we adopt the same radii of source stars and their spots, i.e.  $r_* = 0.05\theta_E$  and  $0.1\theta_E$  and  $r_{\text{spot}} = 0.2r_*$ , and the surface brightness contrast, i.e.  $\mathcal{C} = 10$ . Unlike the single-lens event cases, however, we place the spots at the center of the source stars, i.e.  $s = 0$ , but we will discuss the dependency of the deviation  $\epsilon_b$  on the spot position in the following paragraph. In the lower panels, we also present several light curves for source stars with (solid lines) and without spots (dotted lines). The source star trajectories corresponding to individual light curves are represented

by dot-long dashed lines in the upper panels and each pair of the light curve and trajectory are marked by the same number.

From the figure, one finds following patterns of  $\epsilon_b$ . First, significant deviations in amplification occur at near the regions along the caustics, implying that noticeable deviations in light curves occur when the spot crosses the caustic. If the spot is located at different positions on the source star, the regions for optimal spot detection will change because the spot will cross the caustic at a different time. However, since the spot is confined within the small region of the source star, the change will be very slight. Second, since the significant deviation region well surrounds most of the caustic lines, one can detect the deviation for nearly all caustic-crossing events regardless of the lens trajectories. Third, while the center-to-limb surface intensity variation, which is another important stellar surface structure, produces very smooth deviations in the light curve (e.g. the Galactic bulge event MACHO 97-BLG-28, Albrow et al. 1999a), the deviations caused by the spot are bumpy. Therefore, one can easily separate the deviations in the light curve caused by the spot.

#### 4. Single-Lens Versus Binary-Lens Events

Although both single-lens and binary-lens microlensing events can be used to detect stellar spots, observing caustic-crossing binary-lens events have following relative advantages in detecting spots over the observations of source-transit single-lens events.

First, caustic-crossing binary-lens events are much more common than source-transit single-lens events. Currently, total 11 candidate caustic-crossing binary-lens events have been reported. These include MACHO LMC#1 (Dominik & Hirshfeld 1994, 1996; Rhie & Bennett 1996), OGLE#7 (Udalski et al. 1994), DUO#2 (Alard, Mao, & Guibert 1995), 97-BLG-28 (Albrow et al. 1999a), 98-SMC-1 (Afonso et al. 1998; Albrow et al. 1999b; Alcock et al. 1999), 96-BLG-3, 97-BLG-1, 97-BLG-41, 98-BLG-12, 98-BLG-42, and 99-BLG-28, (<http://darkstar.astro.washington.edu>). On the other hand, only one candidate source-transit single-lens event has been reported (MACHO Alert 95-30, Alcock et al. 1997). In addition, while one can detect the deviations caused by spots for nearly all caustic-crossing events, spot detection for a significant fraction of source-transit single-lens events will be difficult because only almost direct spot-transit events will produce deviations large enough to detect spots.

Second, for a caustic-crossing binary-lens event, the deviations caused by a spot can be measured with precision and high time resolution from followup observations of the event. The deviations in the light curve last only a few hours during the source star transit of the lens (for a single-lens event) or the caustic (for a binary-lens event). Therefore, followup observations with high photometric precision and time resolution will be essential for the detection of stellar spots. For a binary-lens event, the caustic crossing happens twice and thus although the first crossing was missed one can prepare the followup observations of the second crossing. By contrast, since the source transit of a single-lens event cannot be

predicted a priori as well as never repeats, followup observations cannot be performed for an important fraction of these events.

## REFERENCES

- Afonso, C., et al. 1998, *A&A*, 337, 17
- Alard, C., & Guibert, J. 1997, *A&A*, 326, 1
- Alard, C., Mao, S., & Guibert, J. 1995, *A&A*, 300, L17
- Albrow, M. D., et al. 1999a, *ApJ*, 512, 672
- Albrow, M. D., et al. 1999b, *ApJ*, submitted (astro-ph/9811479)
- Alcock, C., et al. 1993, *Nature*, 365, 621
- Alcock, C., et al. 1997, *ApJ*, 491, 436
- Alcock, C., et al. 1999, *ApJ*, 518, 44
- Aubourg, E., et al. 1993, *Nature*, 365, 623
- Dominik, M., & Hirshfeld, A. C. 1994, *A&A*, 289, L31
- Dominik, M., & Hirshfeld, A. C. 1996, *A&A*, 313, 841
- Gaudi, B. S., & Gould, A. 1999, *ApJ*, 513, 619
- Gould, A., & Welch, D. 1996, *ApJ*, 464, 212
- Heyrovský, D., & Sasselov, D. 1999, *ApJ*, submitted (astro-ph/9906024)
- Loeb, A., & Sasselov, D. 1995, *ApJ*, 449, L33
- Maoz, D., & Gould, A. 1994, *ApJ*, 425, L67
- Nemiroff, R. J., & Wickramasinghe, W. A. D. T. 1994, *ApJ*, 424, L21
- Peng, E. W. 1997, *ApJ*, 475, 43
- Rhie, S. H., & Bennett, D. P. 1996, *Nucl. Phys. Proc. Suppl.*, 51B, 86
- Schneider, D., & Weiss, A. 1986, *A&A*, 164, 237
- Stubbs, C. W. 1999, in *Proc. of ASP Conf. 165, The Galactic Halo*, ed. B. K. Gibson, T. S. Axelrod, & M. E. Putman, 503
- Udalski, A., et al. 1993, *Acta Astron.*, 43, 289
- Udalski, A., et al. 1994, *ApJ*, 436, L103
- Valls-Gabaud, D. 1994, in *Large-Scale Structure of the Universe*, ed. J. Muckel et al. (Singapore: World Scientific), 326
- Valls-Gabaud, D. 1998, *MNRAS*, 294, 747
- Witt, H. J. 1990, *A&A*, 263, 311
- Witt, H. J. 1995, *ApJ*, 449, 42

Witt, H. J., & Mao, S. 1994, ApJ, 430, 505



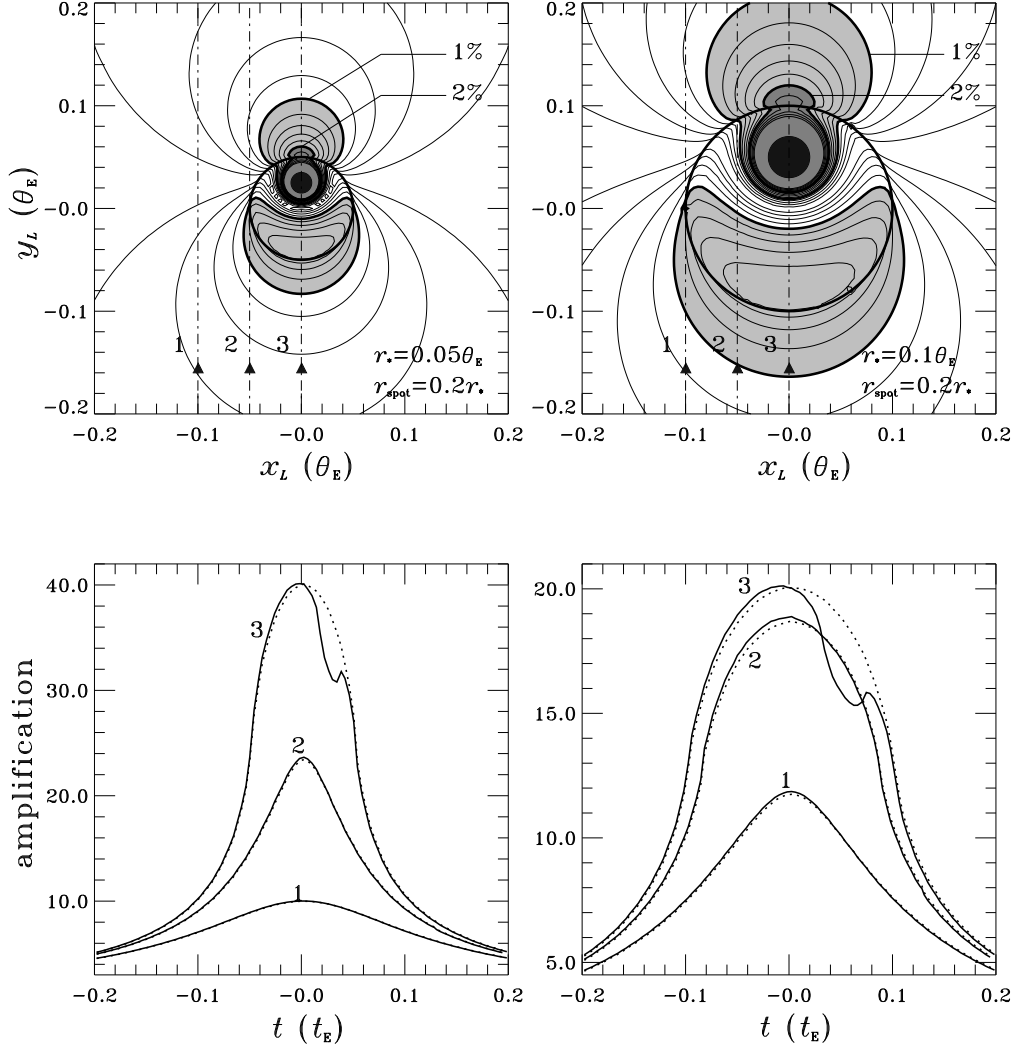


**Figure 1:** Upper panels: contours of the fractional amplification deviation  $\epsilon_s$  as a function of the *lens* position  $(x_L, y_L)$  for single-lens microlensing events. The two circles in each panel represent the source star (big empty circle centered at the origin) and the stellar spot on it (small filled circle), respectively. The source stars have radii of  $r_* = 0.05\theta_E$  and  $0.1\theta_E$ . For both cases, the spot has a relative radius of  $r_s/r_* = 0.2$  and the adopted contrast parameter  $\mathcal{C} = I_*/I_{\text{spot}} = 10$  for both cases. Contours are drawn with a spacing of 0.2% from  $\epsilon_s = 0.2\%$  and the regions with  $\epsilon_s \geq 1\%$  and  $\epsilon_s \geq 2\%$  are shaded by darkening gray tones. Lower panels: the light curves (solid curves) of single-lens microlensing events for source stars with spots. The lens trajectories corresponding to the individual light curves are represented by dot-long dashed lines in the upper panels and each pair of the light curve and trajectory are marked by the same number. The dotted curves represent the light curves which are expected when the source stars have no spot.

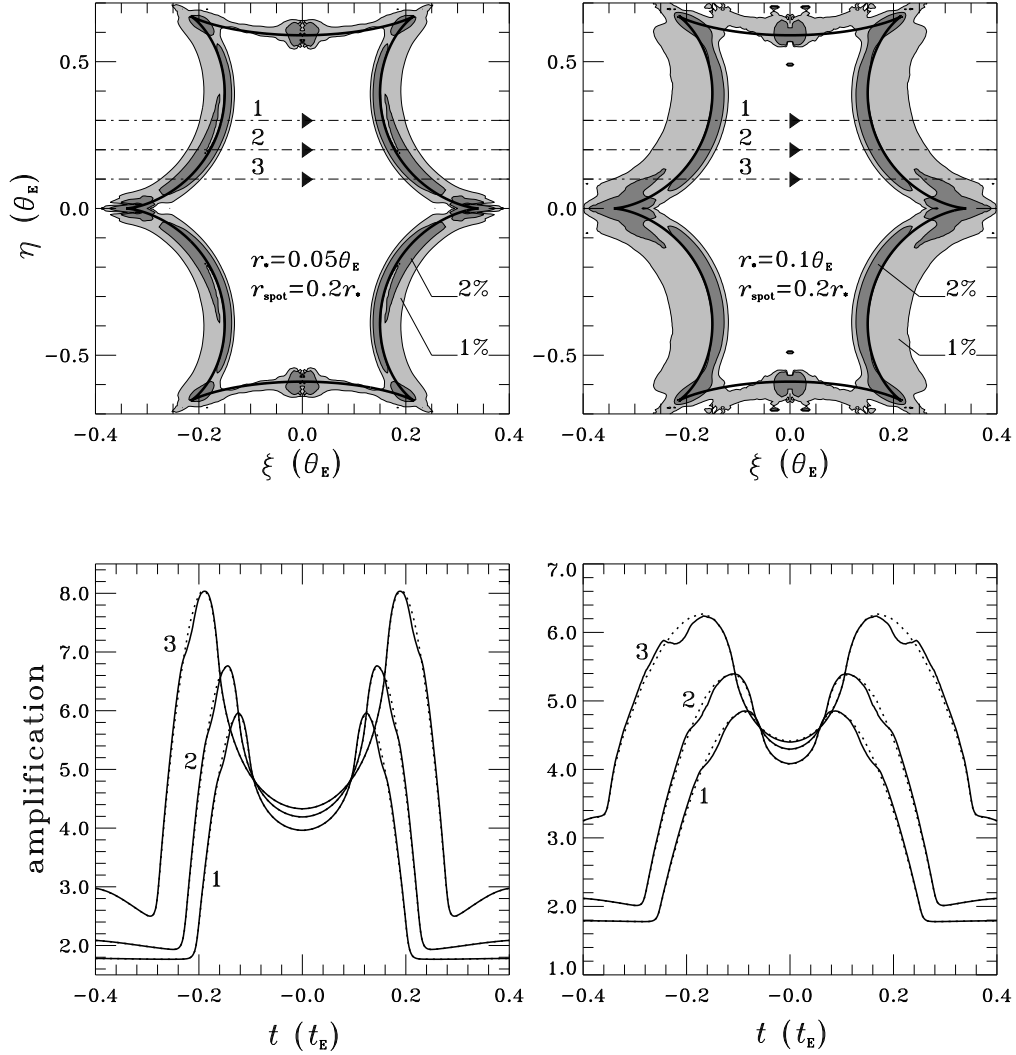


**Figure 2:** Upper panel: contours of amplification deviation  $\epsilon_b$  as a function of the *source star* position  $(\xi, \eta)$  for binary-lens microlensing events. The lens system is composed of equal mass lenses (i.e. mass ratio  $q = 1.0$ ) with a normalized binary separation of  $a = 1.0$ . The closed figure (marked by thick solid curves) in each panel represents the caustics of the binary-lens system. The contours are drawn at the levels of  $\epsilon_b = 1\%$  and  $2\%$  and the regions with  $\epsilon_b \geq 1\%$  and  $\epsilon_b \geq 2\%$  are shaded by darkening gray tones. The radii of source stars and their spots and the surface brightness contrast are same as in Figure 1. Lower panel: the light curves (solid curves) of binary-lens microlensing events for source stars with spots. The source star trajectories corresponding to the individual light curves are represented by dot-long dashed lines in the upper panels and each pair of the light curve and trajectory are marked by the same number. The dotted curves represent the light curves without spots.